JIPB Journal of Integrative Plant Biology

Research Article
https://doi.org/10.1111/jipb.13484

Auxin signaling module OsSK41-OsIAA10-OsARF regulates grain yield traits in rice[oo]

Fuying Ma[1†], Fan Zhang[2,3†*], Yu Zhu[1†], Dengyong Lan[1], Peiwen Yan[1], Ying Wang[1], Zejun Hu[4], Xinwei Zhang[1], Jian Hu[1], Fuan Niu[1,4], Mingyu Liu[1], Shicong He[1], Jinhao Cui[1], Xinyu Yuan[1], Ying Yan[4], Shujun Wu[4], Liming Cao[4], Hongwu Bian[5], Jinshui Yang[1], Zhikang Li[2,3,6*] and Xiaojin Luo[1*]

1. State Key Laboratory of Genetic Engineering and MOE Engineering Research Center of Gene Technology, School of Life Sciences, Fudan University, Shanghai 200438, China
2. Institute of Crop Sciences, Chinese Academy of Agricultural Sciences, Beijing 100081, China
3. College of Agronomy, Anhui Agricultural University, Hefei 230036, China
4. Institute of Crop Breeding and Cultivation, Shanghai Academy of Agricultural Sciences, Shanghai 201403, China
5. Institute of Genetics and Regenerative Biology, Key Laboratory for Cell and Gene Engineering of Zhejiang Province, College of Life Sciences, Zhejiang University, Hangzhou 310058, China
6. Shenzhen Branch, Guangdong Laboratory for Lingnan Modern Agriculture, Genome Analysis Laboratory of the Ministry of Agriculture, Agricultural Genomics Institute at Shenzhen, Chinese Academy of Agricultural Sciences, Shenzhen 518100, China
†These authors contributed equally to this work.
*Correspondences: Xiaojin Luo (luoxj@fudan.edu.cn, Dr. Luo is fully responsible for the distributions of the materials associated with this article); Zhikang Li (lizhikang@caas.cn); Fan Zhang (zhangfan03@caas.cn)

Fuying Ma

Xiaojin Luo

ABSTRACT

Auxin is an important phytohormone in plants, and auxin signaling pathways in rice play key roles in regulating its growth, development, and productivity. To investigate how rice grain yield traits are regulated by auxin signaling pathways and to facilitate their application in rice improvement, we validated the functional relationships among regulatory genes such as *OsIAA10*, *OsSK41*, and *OsARF21* that are involved in one of the auxin (OsIAA10) signaling pathways. We assessed the phenotypic effects of these genes on several grain yield traits across two environments using knockout and/or overexpression transgenic lines. Based on the results, we constructed a model that showed how grain yield traits were regulated by *OsIAA10* and *OsTIR1*, *OsAFB2*, and *OsSK41* and *OsmiR393* in the OsSK41-OsIAA10-OsARF module and by OsARF21 in the transcriptional regulation of downstream auxin response genes in the OsSK41-OsIAA10-OsARF module. The population genomic analyses revealed rich genetic diversity and the presence of major functional alleles at most of these loci in rice populations. The strong differentiation of many major alleles between *Xian/indica* and *Geng/japonica* subspecies and/or among modern varieties and landraces suggested that they contributed to improved productivity during evolution and breeding. We identified several important aspects associated with the genetic and molecular bases of rice grain and yield traits that were regulated by auxin signaling pathways. We also suggested rice auxin response factor (OsARF) activators as candidate target genes for improving specific target traits by overexpression and/or editing subspecies-specific alleles and by searching and pyramiding the 'best' gene allelic combinations at multiple regulatory genes in auxin signaling pathways in rice breeding programs.

Keywords: allele evolution, auxin signaling pathways, *OsARFs*, Os*IAA10*, yield traits

Ma, F., Zhang, F., Zhu, Y., Lan, D., Yan, P., Wang, Y., Hu, Z., Zhang, X., Hu, J., Niu, F., et al. (2023). Auxin signaling module OsSK41-OsIAA10-OsARF regulates grain yield traits in rice. J. Integr. Plant Biol. **00:** 1–15.

INTRODUCTION

Rice (*Oryza sativa* L.) is an important food crop that feeds half the world's population. The rapid global population growth and continued loss of farmlands have posed a great threat to world rice production and food security. To overcome these problems, worldwide rice breeding efforts have been largely focused on improving rice yield potential with two major breakthroughs: first through the development of semi-dwarf rice varieties known as the Green Revolution since the late 1950s, and then by the development of hybrid rice since the late 1970s. However, yield potentials of both inbred and hybrid rice cultivars seem to have reached their respective plateaus since the 1990s, despite the tremendous breeding efforts to break the rice yield ceiling. Meanwhile, global rice functional genomics efforts have achieved tremendous progress with more than 4,600 rice genes having been cloned and functionally characterized (Wing et al., 2018). The recent advances in rice population genomics have revealed extremely rich genomic diversity in the primary gene pool of rice (Wang et al., 2018b; Zhang et al., 2021). Nevertheless, it remains a great challenge to translate this progress in rice functional and population genomics research into applicable breeding strategies/technologies for efficient improvement of complex traits such as rice yields (Li and Zhang, 2013).

Current knowledge indicates that most complex traits in plants, such as grain yield components and tolerance/resistance to abiotic and biotic stresses, are controlled by complex signaling pathways each involving multiple layers of regulatory and downstream genes that act in a complex interactive manner (Zhang et al., 2011). As important components of grain yield and quality with high heritability, traits related to rice grain shape and weight have been a major focus of attention in rice functional genomics research in past decades. To date, at least 22 genes that affect rice grain shape and weight have been cloned (Jiang et al., 2022). Functionally, these grain shape and weight-related genes are involved in pathways such as the ubiquitin-proteasome pathway, G protein signaling pathway, and mitogen-activated protein kinase signaling pathway (Jiang et al., 2022). Auxin is a key phytohormone that plays important roles in rice growth and development (Nakamura et al., 2006), and thus is expected to influence rice grain yield traits. Auxin signaling typically involves an auxin response factor (ARF), an auxin/indole acetic acid (Aux/IAA) protein, and a transcription factor as its key functional components (Müllender et al., 2021). For example, the TIR1/AFB F-BOX is an auxin co-receptor transcription factor that senses signals from auxin and promotes its degradation through ubiquitination via its binding of an SCF E3 ligase, TIR1/AFB, to domain II of the Aux/IAA protein (Gray et al., 2001). In rice and other cereals, some auxin-indole-3-acetic acids (*IAAs*) such as *OsIAA29* and *OsIAA10* are specifically expressed and accumulated in high concentrations at the early stage of grain development (Jin et al., 2016; Basunia et al., 2021), but how these *IAAs* regulate the development of rice yield traits remains unclear. Ishimaru et al. (2013) reported a rice quantitative trait locus (QTL) gene, *TGW6*, that encoded IAA-glucose hydrolase and limited the cell number and length of rice grains by controlling the supply of IAAs. Similarly, a diverse group of plant GSK3-like kinases is known to play various roles in plant growth, development, and stress responses (Youn and Kim, 2015; Wang et al., 2018a). In rice, *OsGSK1*, *OsGSK2*, *OsGSK3*, and *OsGSK4* are homologs of an *Arabidopsis* gene, *BRASSINOSTEROID-INSENSITIVE 2* (*BIN2*), that plays an important role in the brassinosteroid signaling pathway and negatively regulates the expression of brassinosteroid-responsive downstream genes. Loss of *OsGSK3* function resulted in significant increases in grain length (GL) and grain weight (GW) (Gao et al., 2019). Overexpression of *OsGSK2* resulted in small grains, while downregulation of *OsGSK2* expression resulted in long grains (Tong et al., 2012; Lyu et al., 2020). Previously, we cloned a major QTL gene (*OsSK41*/*OsGSK5*) that encoded GSK3/SHAGGY-Like Kinase 41, which negatively regulated grain size and weight (Hu et al., 2018). Many genes involved in auxin signaling pathways influence rice grain yield traits; however, the functional relationships among these genes are complex, and how these functional relationships are related to their effects on complex grain yield traits is unclear. Rice genes are known to vary considerably in their genetic diversity in rice populations (Zhang et al., 2021), but it remains unclear what implications the population genomic parameters of different genes in auxin signaling pathways have for their potential applications in rice yield improvement.

In this study, we addressed these two questions by validating the functional relationships of several regulatory genes in an auxin (OsIAA10) signaling pathway and assessing their phenotypic effects on rice grain and yield traits. The results led us to a general model as the genetic and molecular bases of complex traits regulated by auxin signaling pathways. We also demonstrated how natural alleles at these genes were distributed in different rice populations and their associations with rice grain yield traits. Our results suggest general strategies for how to integrate information from functional and population genomics research for the efficient improvement of complex traits through accurate selection and manipulation of target genes for improving complex traits with various molecular breeding strategies.

RESULTS

Evidence for the direct interaction between OsSK41 and OsIAA10

In our previous work, *OsSK41* was confirmed as one of the key factors that determines rice grain size and weight. Overexpression of *OsSK41* reduced GL and GW, and *OsSK41* knockout lines had longer and heavier grains (Hu et al., 2018). To further understand how *OsSK41* regulates rice grain development, we performed yeast two-hybrid (Y2H) screening using a normalized rice cDNA prey library and identified

OsIAA10 interacted with OsSK41. This finding was verified by the direct interaction between their full-length protein-coding sequences (CDSs) (Figure S1). OsIAA10 is known to have four functional domains, I–IV. To determine which of the OsIAA10 functional domains interacted with OsSK41, we constructed a series of AD fusion vectors according to the distribution of the functional domains of OsIAA10 in the Y2H assays. The results indicated that domain II of OsIAA10 was required for its interaction with OsSK41 (Figure 1A). The interaction between OsIAA10 and OsSK41 was verified *in vivo* in a split-luciferase (LUC) assay, in which LUC activity was detected only in the co-expressed region of cLUC-OsSK41 and OsIAA10-nLUC, but not in regions of cLUC and nLUC, cLUC-OsSK41 and nLUC, or cLUC and OsIAA10-nLUC in tobacco leaves (Figure 1B). In the *in vitro* pull-down assay, His-OsIAA10 was pulled down by glutathione S-transferase (GST)-OsSK41 (Figure 1C), indicating OsIAA10 interacted directly with OsSK41. Similar to OsSK41 (Hu et al., 2018), OsIAA10 also localized in the

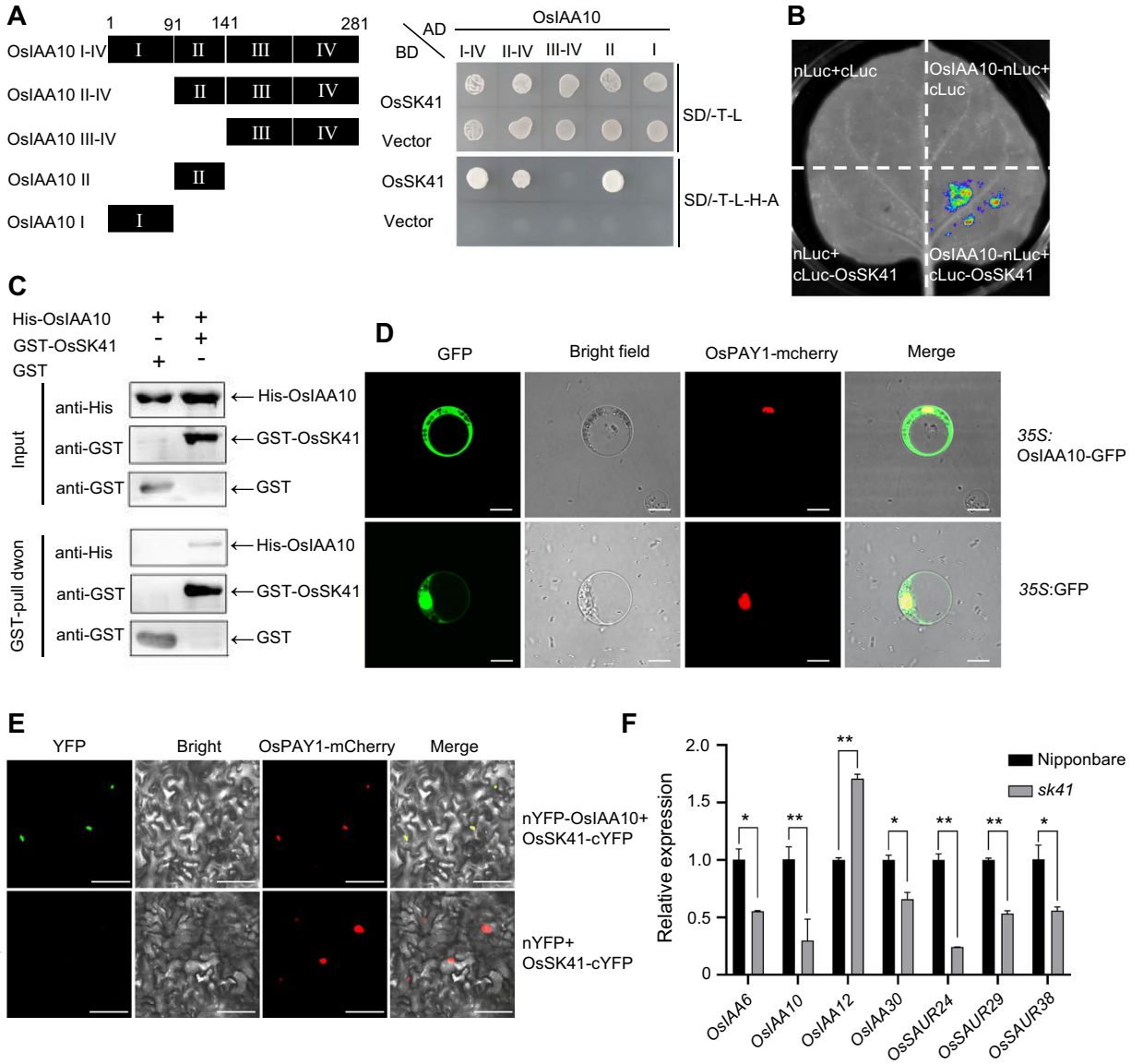

Figure 1. Experimental evidence for the interaction between OsSK41 and OsIAA10

(**A**) Yeast two-hybrid assays. OsSK41 was fused with the DNA-binding domain (BD) of GAL4, and full-length and various truncated forms of OsIAA10 were fused with the activation domain (AD) of GAL4. (**B**) Verification of the *in vivo* interaction between OsSK41 and OsIAA10 by the split-luciferase assay. Split-luciferase assays. OsSK41 and OsIAA10 were fused with either the C-terminal (cLUC) or N-terminal (nLUC) portion of firefly luciferase (LUC). (**C**) Pull-down assay confirmation of the *in vitro* interaction of OsIAA10 and OsSK41. (**D**) Subcellular localization of OsIAA10 in rice protoplasts shown in scale bars of 20 μm. (**E**) BiFC assay demonstration of the interaction of OsSK41 with OsIAA10 in the nucleus of the Tabaco leaf, as shown in scale bars of 50 μm. (**F**) qRT-PCR verification of the relative expression of seven auxin response factors in the *OsSK41* knockout lines and wild-type Nipponbare at the booting stage of rice. The data are shown as means ± *SEM* ($n = 3$), where * and ** indicate the significance levels of $P < 0.05$ and 0.01 according to Student's *t*-tests, respectively.

cytoplasm and nucleus of rice protoplasts (Figure 1D), but their interaction occurred in the nucleus as determined by a bimolecular fluorescence complementation (BiFC) assay (Figure 1E).

To understand how the interaction between OsSK41 and OsIAA10 influenced the expression of *OsIAA10* and its downstream genes, we performed an RNA sequencing analysis using the young panicles of wild-type Nipponbare rice and *OsSK41* knockout lines at the booting stage. Compared with wild-type Nipponbare, 1,774 differentially expressed genes (DEGs) were detected in the *OsSK41* knockout lines; 1,113 were up-regulated and 661 were down-regulated (Figure S2A). Kyoto Encyclopedia of Genes and Genomes pathway enrichment analysis showed that these DEGs were enriched mainly in metabolic pathways and biosynthesis of secondary metabolites (Figure S2B). The down-regulated DEGs included many auxin-responsive genes such as *OsIAA6*, *OsIAA10*, *OsIAA12*, *OsIAA30*, *OsSAUR24*, *OsSAUR29*, and *OsSAUR38*, which were validated by quantitative real-time polymerase chain reaction (qPCR) (Figure 1F). Because different rice IAA proteins have similar functional domains, this result suggested that OsSK41 interacted with multiple OsIAAs that regulate the expression of large numbers of downstream genes involved in metabolic pathways and biosynthesis of secondary metabolites.

OsIAA10 negatively regulates GL and GW

To explore the function of *OsIAA10*, we examined the expression pattern of *OsIAA10* in wild-type Nipponbare and detected its expression in roots and leaves at the seedling stage and in roots, stems, and leaves at the booting stage (Figure S3), suggesting that *OsIAA10* has a wide range of functions. To determine how *OsIAA10* affects rice grain and yield traits, we constructed a CRISPR/Cas9 *OsIAA10* knockout vector and transformed it into wild-type Nipponbare and Zhonghua 11 (ZH11) via *agrobacterium*-mediated assay (Figures 2A, S4A, S5A). The *OsIAA10* knockout lines had significantly longer and heavier grains than corresponding wild-type under the normal long-day environment in Shanghai and short-day environment in Hainan, though their grain width (GW) was slightly reduced (Figures 2B, C, E; S4B, C; S5B–D). To determine whether the expression level of *OsIAA10* affected the grain traits, we constructed a *35S*::*OsIAA10* vector and introduced it into the Nipponbare background. *OsIAA10* overexpressing lines had significantly reduced GL, GW, thousand grain weight (TGW), and plant height (PH) compared with these traits in wild-type Nipponbare (Figure 2C–F), indicating *OsIAA10* may suppress both plant and grain development of rice. Using a scanning electron microscopy, we observed significantly increased cell length in the outer glume region of rice grains in the *OsIAA10* knockout lines, and the opposite was true in the *OsIAA10* overexpressing lines (Figure 2G, H), indicating *OsIAA10* negatively regulated grain size and weight by limiting the expansion of rice outer glume cells.

OsSK41 phosphorylates OsIAA10 and modulates the stability of the OsIAA10 protein

Because OsSK41 has kinase activity and interacts with OsIAA10, we examined whether OsSK41 could phosphorylate OsIAA10 via an *in vitro* phosphorylation experiment. As expected, phosphorylated His-OsIAA10 was detected in the presence of ATP, but not without ATP, indicating that OsSK41 phosphorylated OsIAA10 *in vitro* (Figure 3A). The liquid chromatography with tandem mass spectrometry (LC-MS/MS) analysis identified four sites in OsIAA10 phosphorylated by OsSK41; two were located in domain II and two were located in domain I of OsIAA10 (Figure 3B). Our results suggested that phosphorylation of OsIAA10 by OsSK41 enhanced the stability of the OsIAA10 protein (Figure 3C). Indeed, the *in vitro* phosphorylation experimentindicated that the unphosphorylated His-OsIAA10 protein degraded faster than the pre-phosphorylated His-OsIAA10 protein (Figure 3C). Domain II of the Aux/IAA protein is required for the characteristic rapid degradation (Worley et al., 2000). Furthermore, when the phosphorylation sites of OsIAA10 at Domain II were mutated to alanine to prevent its phosphorylation by OsSK41, the mutated OsIAA10-M maintain its protein stability (Figure 3D). This is consistent with the result of the β-galactosidase experiment, which showed that the interaction between OsIAA10-M and OsSK41 was weakened (Figure 3E, F), confirming that the two phosphorylation sites on domain II were critical for OsSK41 to stabilize OsIAA10. To determine the genetic relationship between *OsSK41* and *OsIAA10*, we created a double mutant, *sk41*/*iaa10*. The phenotypic effects of *sk41*/*iaa10* which caused longer and heavier grains, were the same as those of single *sk41* mutant, but greater than those of single *iaa10* mutant (Figure 3G, H), indicating that *OsIAA10* was the downstream target gene of *OsSK41*.

Functional characterization of *OsTIR1*, *OsAFB2*, and *OsARF21*

Rice genes *OsTIR1*, *OsARF6*, *OsARF11*, *OsARF12*, *OsARF17*, *OsARF21*, and *OsARF25* are known to regulate plant growth and development through their interactions with OsIAA10 (Jin et al., 2016; Qin et al., 2020). In rice, OsTIR1 (F-box transport inhibitor response 1) and its homolog OsAFB2 (auxin signaling F-box receptor) form a co-receptor complex that binds domain II of Aux/IAA proteins to trigger their ubiquitination and degradation (Guo et al., 2021). Both *OsTIR1* and *OsAFB2* are negatively regulated by the microRNA *OsmiR393* (Bian et al., 2012; Xia et al., 2012). OsARF6, OsARF11, OsARF12, OsARF17, OsARF21, and OsARF25 are auxin response transcription factors that interact with domains III and IV of Aux/IAA proteins to regulate the downstream genes of the auxin signaling pathway (Shen et al., 2010). To understand how these transcription factor genes influence rice grain and yield traits through their interactions with OsIAA10, we created knockout mutants for *OsTIR1*, *OsAFB2*, and *OsARF21*, as well as *OsmiR393* overexpression lines. Using these transgenic lines (Figure 4A, D), we validated the interactions of OsIAA10

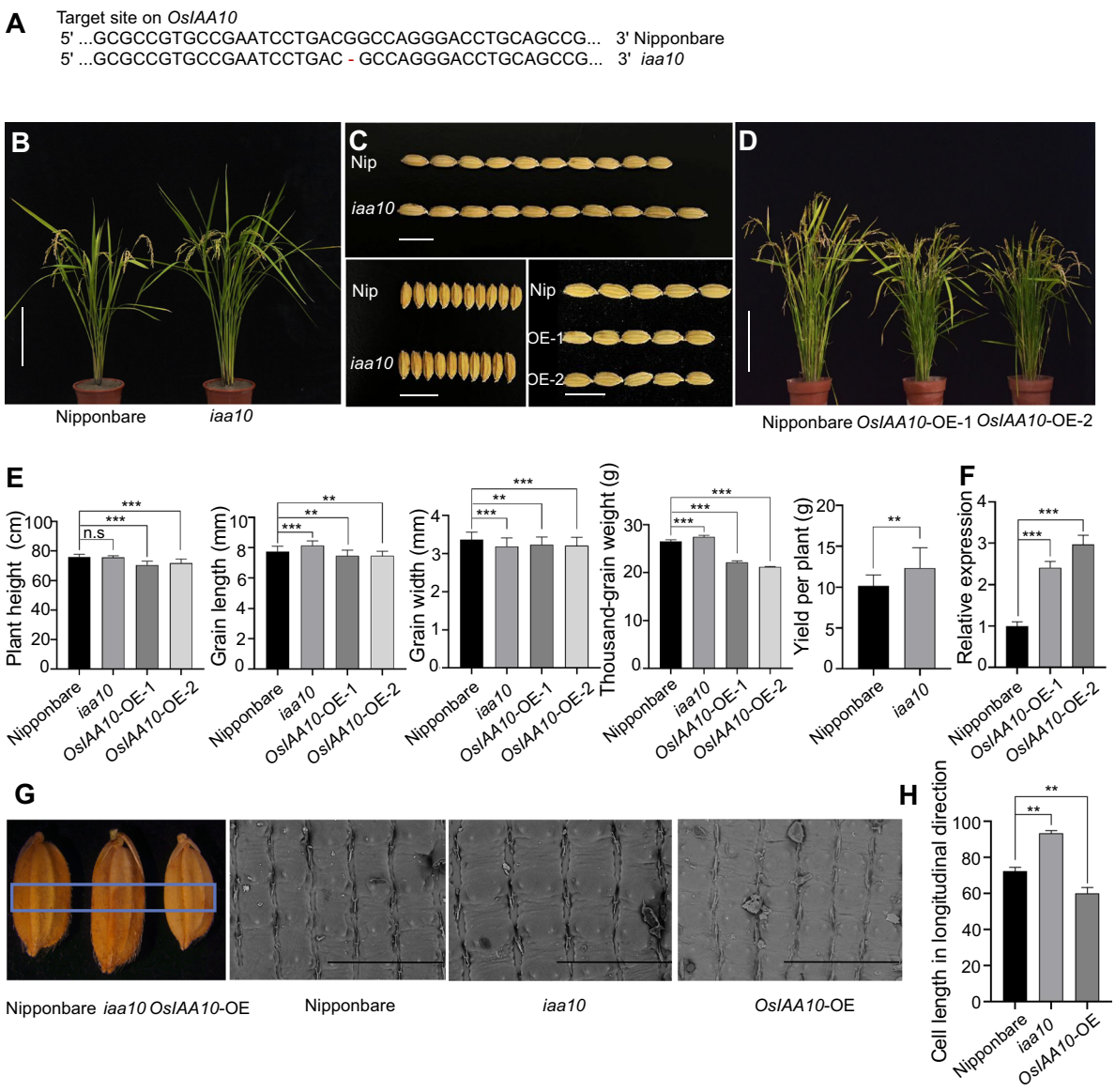

Figure 2. Phenotypic effects of *OsIAA10* on rice grain traits and plant height in transgenic knockout and overexpression lines in Shang Hai

(**A**) The knockout target of the *OsIAA10* knockout lines in the wild-type Nipponbare background. (**B**) Phenotypic comparison between the wild-type Nipponbare and *OsIAA10* knockout lines, shown in scale bars of 30 cm. (**C**) Grain phenotypes of wild-type Nipponbare, *OsIAA10* knockout lines and *OsIAA10* overexpressing lines, shown in scale bars of 10 mm. (**D**) Phenotypic comparison of wild-type Nipponbare and *OsIAA10* overexpressing lines, shown in scale bars of 30 cm. (**E**) Phenotypic differences in plant height and grain traits between wild-type Nipponbare and *OsIAA10* knockout lines and *OsIAA10* overexpression lines. (**F**) The relative expression levels of two *OsIAA10* overexpression lines as compared with wild-type Nipponbare. (**G**) The scanning electron microscope observation and comparison of the outer surfaces of rice seed glumes among wild-type Nipponbare, *OsIAA10* knockout lines and *OsIAA10* overexpressing lines at mature grain stage. The blue box highlights the area used to compare the longitudinal length of cells of wild-type Nipponbare, *OsIAA10* knockout lines and *OsIAA10* overexpressing lines. scale bars: 200 μm. (**H**) Comparison of cell lengths of seed glume in wild-type Nipponbare, *OsIAA10* knockout lines and *OsIAA10* overexpressing lines. The data are shown as means ± *SEM* ($n = 10$ in **E**; $n = 3$ in **F** and **H**). In **E**, **F** and **H**, n.s, ** and *** indicate no significant difference, and significant differences at levels of $P < 0.01$ and 0.001, respectively, according to Student's *t*-tests.

with OsTIR1 in the nucleus by BiFC assays (Figure 4F, G), consistent with a previous report (Jin et al., 2016). In the Shanghai and Hainan experiments, the *OsTIR1* and *OsAFB2* knockout lines, when compared with wild-type Nipponbare, showed significantly reduced GL, GW, and TGW, though the phenotypic effects of *OsTIR1* were significantly greater (Figures 4B, C, E and S6). As expected, the phenotypic effects of the *OsmiR393* overexpression lines on the grain traits were approximately equal to the summed effects of *OsTIR1* knockout lines and *OsABF2* knockout lines, consistent with the regulatory role of *OsmiR393*. Also, the *OsTIR1* knockout lines showed significantly reduced PH, panicle length (PL), panicle number per plant (PN), spikelet in main panicle (SMP), and grain yield per plant (GYP) in the Hainan experiment, and

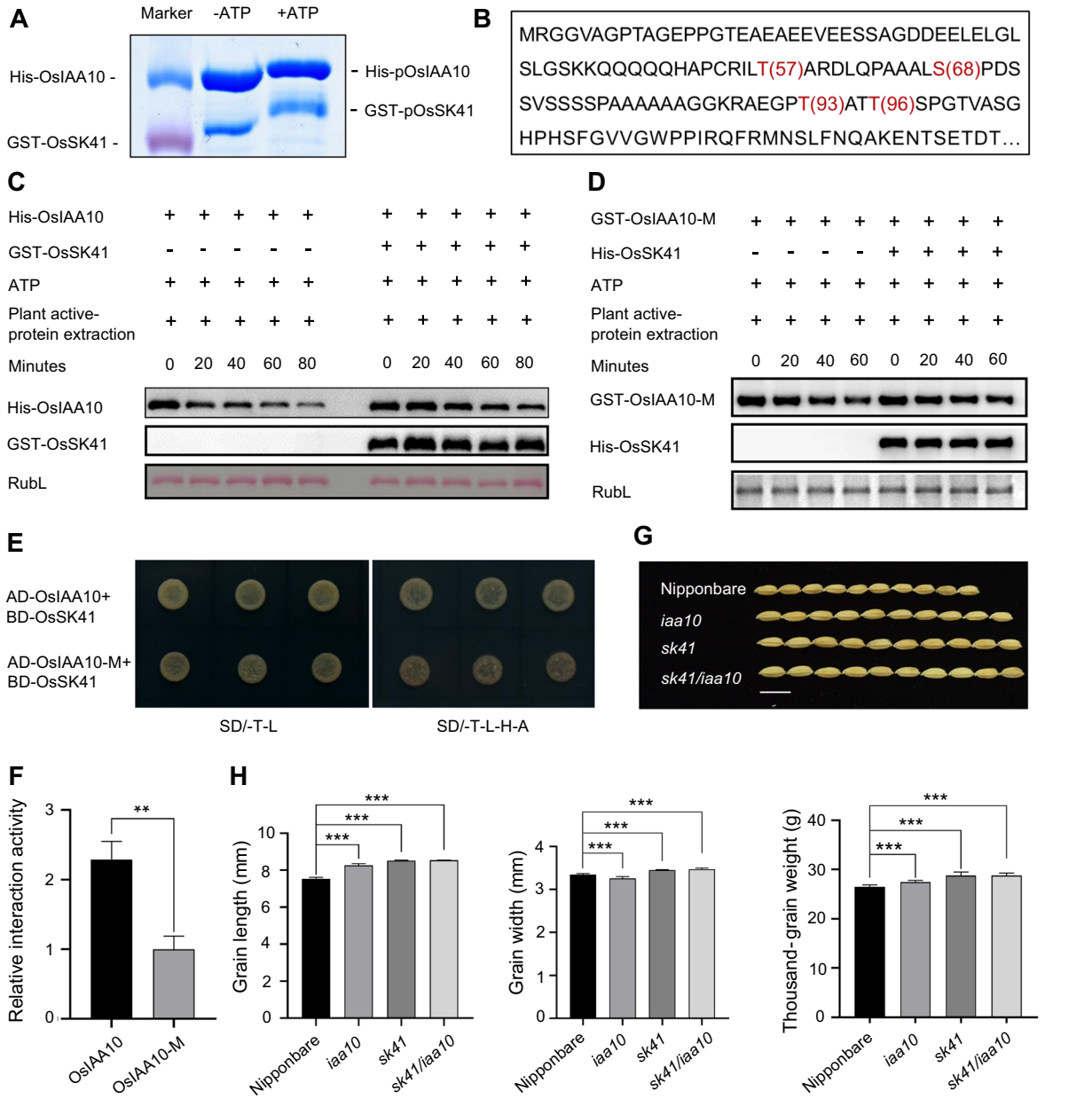

Figure 3. Experimental evidence for the phosphorylation OsIAA10 by OsSK41 in rice

(**A**) *In vitro* experimental verification of phosphorylation of OsIAA10 by OsSK41.His-OsIAA10 migration rate slows down after the addition of GST-OsSK41 when phos-tag is added to the protein gel. (**B**) The mass spectrometry analysis results showing the four sites in OsIAA10 phosphorylated by OsSK41 (marked in red). (**C**) *In vitro* verification of OsIAA10 being degraded slowly after phosphorylated by OsSK41. (**D**) *In vitro* verification of the mutated OsIAA10-M phosphorylated by OsSK41 showing no significant change in its degradation rate (the two sites of OsIAA10 at domain II phosphorylated by OsSK41 were mutated to alanine and represented by OsIAA10-M). (**E**) The yeast two-hybrid verification of the interaction between OsIAA10 or mutated OsIAA10-M and OsSK41. (**F**) The relative strengths of the interaction between OsIAA10 and mutated OsIAA10-M with OsSK41 based on the β-galactosidase activity assay. (**G**) Comparison of grain phenotypes between the wild-type Nipponbare, *OsIAA10* knockout lines, *OsSK41* knockout lines and sk41/iaa10 mutant lines. (**H**) Comparison of grain traits between the wild-type Nipponbare, *OsIAA10* knockout lines, *OsSK41* knockout lines and *sk41/iaa10* double-mutant lines. The data are shown as means ± *SEM* ($n = 3$ in **F**; $n = 10$ in **H**). In **F** and **H**, ** and *** indicated significant differences at levels of $P < 0.01$ and 0.001, respectively, according to Student's *t*-tests.

so did *OsABF2* knockout lines for the same traits except for PN (Figure S6). These results suggested that *OsTIR1* and *OsAFB2* have similar and independent functions on rice growth and development, and their functional differentiation was quantitative rather than qualitative; furthermore, their effects on the measured grain traits were consistent with those reported previously (Jin et al., 2016). Similar to OsSK41 (Figure 1A), OsTIR1 interacted with domain II of OsIAA10 (Jin et al., 2016), but OsTIR1 did not interact directly with OsSK41 (Figure S7). These observations suggested possible

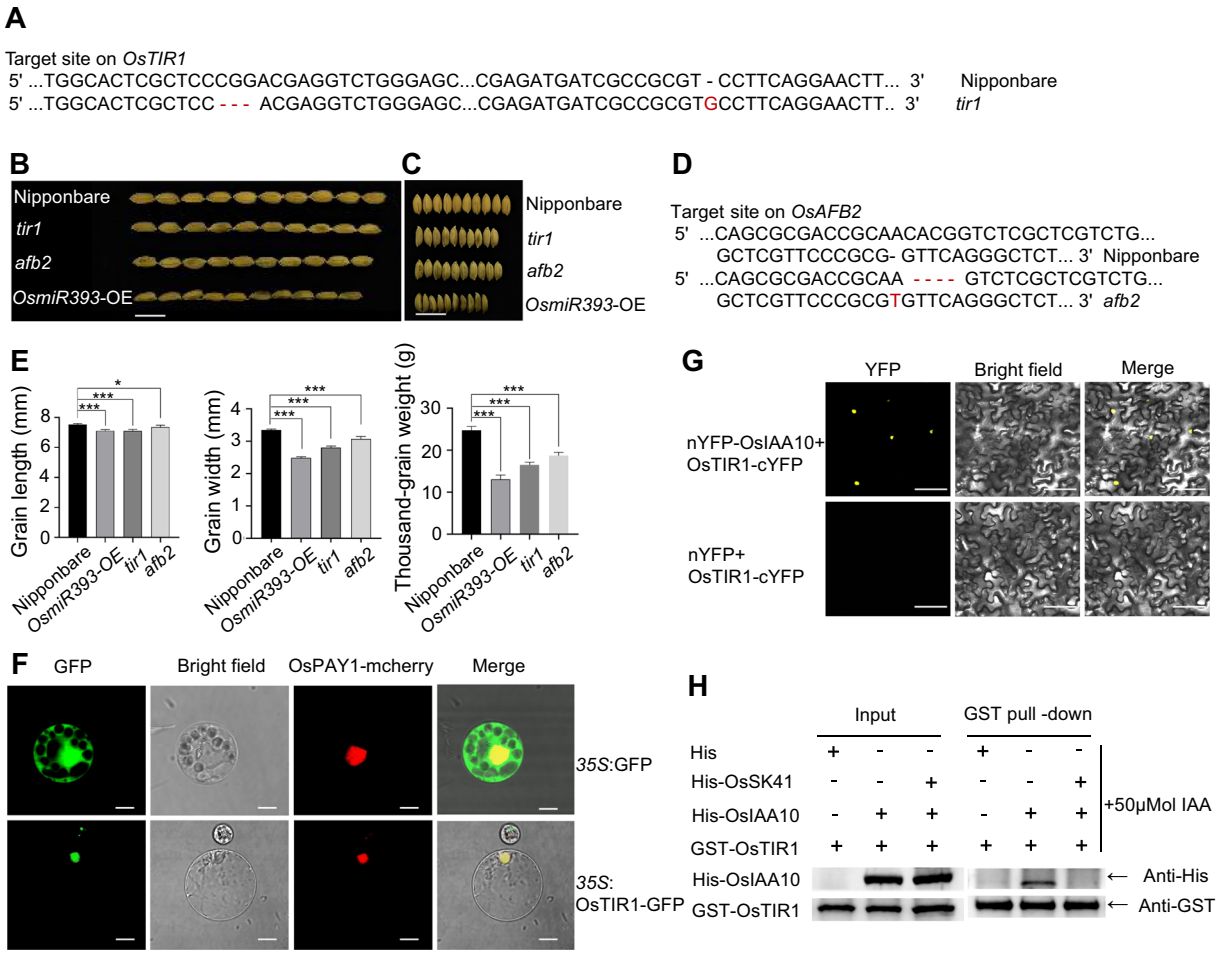

Figure 4. OsTIR1 interacts with OsIAA10 to regulate granulotype and is interfered by OsSK41

(**A**) The knockout target of *OsTIR1* in the wild-type Nipponbare background. (**B**) and (**C**) Grain-type comparison of the wild type Nipponbare, *OsTIR1* knockout lines, *OsAFB2* knockout lines and *OsmiR393* overexpression lines, shown in scale bars of 10 mm. (**D**) The knockout targets of *OsAFB2* in the Nipponbare background. (**E**) Comparison of grain phenotypes among the wild-type Nipponbare, *OsTIR1* knockout lines, *OsAFB2* knockout lines and *OsmiR393* overexpression lines. The data are shown as means ± *SEM* ($n = 10$), and where * and *** indicate statistical significance at $P < 0.05$ and $P < 0.001$, respectively, according to Student's *t*-tests. (**F**) Subcellular localization of OsTIR1 in rice protoplasts, shown in scale bars of 20 μm. (**G**) Bimolecular fluorescence complementation assay confirmation of the interaction between OsTIR1 and OsIAA10 in the nucleus, shown in scale bars of 50 μm. and (**H**) GST-pull down confirmation for the disrupted interaction between *OsTIR1* and *OsIAA10* by *OsSK41*.

competition between OsSK41 and OsTIR1 and/or OsAFB2 in their interactions with OsIAA10. To test this hypothesis, we performed an *in vitro* pull-down assay using purified His-OsSK41, His-OsIAA10, and GST-OsTIR1 in *Escherichia coli*. Using an anti-His antibody and anti-GST antibody in the system, we detected pull down of His-OsIAA10 by GST-OsTIR1, whereas the interaction between His-OsIAA10 and GST-OsTIR1 was disrupted by His-OsSK41 (Figure 4H).

The Y2H evidence for the direct interactions between OsIAA10 and OsARF6, OsARF11, OsARF12, OsARF17, OsARF21, or OsARF25 in plant nuclei is shown in Figure S8 and S9. The *OsARF21* knockout lines showed significantly reduced GL, GW, TGW, PH, and PN, significantly increased SMP, but no significant differences for PL and GYP compared with these traits in wild-type Nipponbare. The overexpression lines *OsARF21-OE* showed significantly increased GL, TGW, and GW, significantly reduced PN, and no significant differences for PL and SMP compared with these traits in wild-type Nipponbare (Figures S10, S11, S12). These results indicated that *OsARF21* positively regulated GL, GW, and TGW, but not GYP. In addition, yeast three-hybrid and β-galactosidase assays showed that OsSK41 was not directly related to OsARF21 (Figure S13), suggesting the interaction between OsSK41 and OsIAA10 did not inhibit the binding of OsIAA10 to OsARFs.

On the basis of these results, we constructed a functional model to show how the genes that functioned at different layers in the OsSK41-OsIAA10-OsARF module influenced different rice yield traits (Figure 5). Briefly, when the concentration of the OsIAA10 protein is high, the receptor complex OsTIR1/OsAFB2 and OsSK41 both interact with domain II of OsIAA10 and compete for OsIAA10, resulting in OsTIR1 ubiquitination to degrade OsIAA10, releasing a unique set of OsARFs (OsARF11, OsARF21,

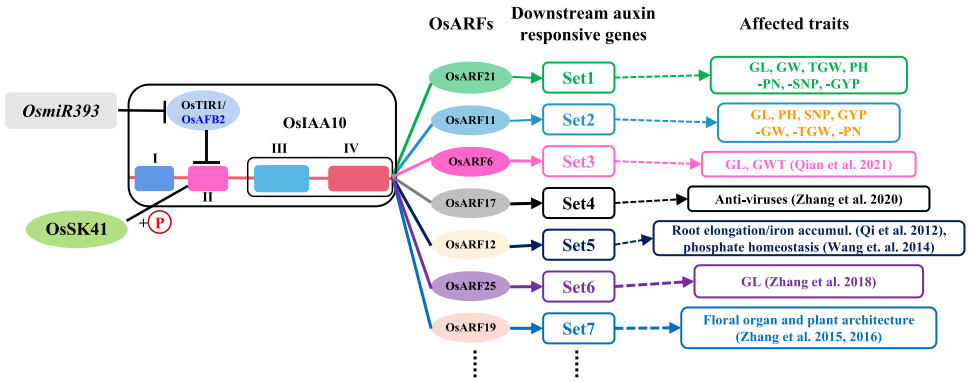

Figure 5. A function model showing how different regulatory genes in the OsSK41-OsIAA10-OsARF module influence different sets of complex traits of rice.

OsARF6, OsARF12, OsARF17, and OsARF25), each of which regulates a unique set of downstream auxin response genes that affect a different suit of complex traits through largely unknown metabolomic/biosynthesis and cellular pathways during rice growth and development. The phenotypic effects of OsSK41 are achieved by inhibiting the degradation of OsIAA10 through phosphorylation, thereby inhibiting the release of the OsARFs, and indirectly repressing expression of their positively regulated downstream auxin-responsive genes and/or metabolomic and biosynthetic pathways. This is true for *OsmiR393*, which affects the grain yield traits through its direct regulation of the OsTIR1/OsAFB2 complex. Clearly, the observed phenotypic effects of the regulatory genes (*OsSK41*, *OsTIR1*, *OSAFB2*, and *OsIAA10*) in the TIR1/AFB/Aux/IAA10 complex on the grain yield traits were achieved primarily through at least one independent set of downstream genes or pathways regulated by OsARF21; however, the downstream gene sets and traits regulated by OsARF6, OsARF11, OsARF12, OsARF17, and OsARF25 remain to be characterized. Thus, the model shows the presence of at least three layers of regulation of rice yield traits by the auxin signaling pathway: OsIAA10 signaled by OsSK41, and OsTIR1/OsAFB2 for the releasing of the OsARFs; transcriptional regulation of large numbers of downstream genes or pathways by the OsARFs, and regulation of complex traits by specific downstream genes/pathways.

Genetic diversity of nine regulatory genes involved in the OsSK41-OsIAA10-OsARF module

To determine the possible application of the genes in the OsSK41-OsIAA10-OsARF module described above to rice improvement, we analyzed the CDS (gcHap) and gene promoter haplotype (gpHap) diversity of these genes in the 3,000 rice genome (3KRG) dataset and major *Xian/indica* and *Geng/japonica* rice populations (Tables S3, S4). *OsIAA10* and *OsARF25* showed a relatively high level of diversity (Shannon's equitability, $E_H = 0.217$ and 0.212) in 3KRG and all major rice populations, whereas *OsARF17*, *OsTIR1*, and *OsAFB2* had relatively low levels of diversity ($E_H = 0.148$, 0.104, and 0.112, respectively) (Table S3), and *OsSK41*, *OsARF12*, and *OsARF21*, which are evolutionarily conserved, had very low levels of diversity ($E_H = 0.069$, 0.043, and 0.019, respectively).

We then examined major haplotype combinations in ≥30 rice accessions by combining the gpHaps with gcHaps (haplotype ID: gpHap_gcHap) of these genes from 3KRG. We identified 11, 13, 8, 10, and 4 major haplotypes for *OsSK41*, *OsIAA10*, *OsTIR1*, *OsAFB2*, and *OsARF21*; the exception was *OsARF11*, which had only a single predominant haplotype in all the rice populations analyzed. Using the reported phenotypic data of grain traits from 3KRG (Niu et al., 2021), we detected significant associations of the major haplotype for *OsSK41*, *OsIAA10*, *OsTIR1*, *OsAFB2*, and *OsARF21* with TGW, GL, GW, and RLW (ratio of length/width) (Figures S14–S18). The phenotype variation explained by each of the genes was 1.3%–17.7% for TGW, 2.0%–10.9% for GL, 0.8%–26.1% for GW, and 1.5%–16.3% for RLW. Among them, *OsIAA10* had the highest phenotype variation explained for all four grain traits, whereas *OsARF21* had the lowest phenotype variation explained. The major haplotype combinations of haplotypes in the gene promoter regions and gcHaps were associated more strongly with the grain traits than either the gpHaps or gcHaps alone, suggesting that the gene expression level may also have contributed to the values of the grain traits in rice.

Artificial selection during modern rice breeding is expected to have impacted the genetic diversity of genes that influence traits associated with rice productivity. To understand if and how this happened for the six genes involved in the OsSK41-OsIAA10-OsARF module, we compared the frequencies of major haplotype combinations between the landraces and modern varieties of populations *Xian/indica* and *Geng/Japonica*. In population *Xian/indica*, haplotype combinations (The superscript of haplotype combination for each gene is composed of two parts: the promoter haplotype ID and CDS haplotype ID, which are connected to each other by an underscore) $OsSK41^{Hap7\_Hap1}$, $OsIAA10^{Hap6\_Hap5}$, $OsIAA10^{Hap4\_Hap1}$, $OsTIR1^{Hap7\_Hap1}$, $OsAFB2^{Hap1\_Hap2}$, and $OsARF21^{Hap3\_Hap1}$ were apparently favored by the artificial selection based on their significantly increased frequencies in modern

varieties compared with their frequencies in landraces (Figures S14–S18). These increased frequencies were at the expense of the significantly decreased frequencies of haplotype combinations *OsIAA10*$^{Hap5\_Hap1}$ and *OsTIR1*$^{Hap1\_Hap1}$ in modern varieties in the same comparison. In population *Geng/japonica*, haplotype combinations *OsSK41*$^{Hap3\_Hap1}$, *OsSK41*$^{Hap10\_Hap2}$, *OsIAA10*$^{Hap3\_Hap3}$, *OsIAA10*$^{Hap4\_Hap1}$, *OsTIR1*$^{Hap7\_Hap1}$, and *OsAFB2*$^{Hap10\_Hap2}$ were favored by artificial selection, whereas the frequencies of haplotype combinations *OsSK41*$^{Hap7\_Hap1}$, *OsSK41*$^{Hap1\_Hap1}$, *OsIAA10*$^{Hap11\_Hap4}$, *OsAFB2*$^{Hap1\_Hap1}$ and *OsAFB2*$^{Hap2\_Hap2}$ were decreased in the same comparison. When a haplotype combination at a locus associated with the highest value of a grain trait was considered as the favorable allele, *OsSK41*$^{Hap7\_Hap1}$, *OsSK41*$^{Hap3\_Hap1}$, *OsIAA10*$^{Hap11\_Hap4}$, *OsIAA10*$^{Hap10\_Hap4}$, *OsTIR1*$^{Hap2\_Hap1}$, and *OsAFB2*$^{Hap2\_Hap2}$ were the favorable haplotypes for TGW in population *Geng/japonica*. Similarly, *OsSK41*$^{Hap4\_Hap1}$, *OsIAA10*$^{Hap6\_Hap5}$, *OsTIR1*$^{Hap1\_Hap1}$, *OsAFB2*$^{Hap7\_Hap1}$, *OsAFB2*$^{Hap6\_Hap1}$, and *OsARF21*$^{Hap3\_Hap1}$ were the favorable haplotypes for TGW in population *Xian/indica*. Cluster analysis based on these favorable haplotypes for TGW (Figure S19) identified the same relationship among these genes as is shown in the model in Figure 5, with *OsSK41*, *OsAFB2*, and *OsTIR1/OsAFB2* acting upstream and *OsIAA10* and *OsARF21* acting downstream in the OsSK41-OsIAA10-OsARF module. Moreover, the haplotype combinations clearly separated the *Xian/indica* and *Geng/japonica* accessions with high TGW, indicating that the haplotypes associated with high TGW were different in these two subspecies populations (Figure S19). For example, *OsIAA10*$^{Hap11\_Hap4}$ with high TGW and GW was enriched mainly in *GJ-sbtrp* accessions, whereas *OsIAA10*$^{Hap7\_Hap4}$ with low TGW and GW was enriched mainly in *Xian/indica* accessions. *OsIAA10*$^{Hap4\_Hap1}$, mainly in *XI-1B* accessions, had significantly longer grains than *OsIAA10*$^{Hap5\_Hap1}$, which was mainly in *XI-2* accessions. These results suggest that most, if not all, major haplotype combinations at these loci in the OsSK41-OsIAA10-OsARF module have gone through strong natural and/or artificial selection during evolution and/or modern breeding, and thus have contributed to the adaptation of the two major rice subspecies to their environments during evolution, and to the increased productivity of modern *Xian/indica* and *Geng/Japonica* cultivars.

DISCUSSION

Current information on rice gene functionality has been built primarily from functional genomic research to link genetic variants of single loci with phenotypic variation of one or more complex traits. Clearly, there is a huge knowledge/information gap between genetic variants of single loci and phenotypic variation of complex traits; i.e., almost all complex traits are controlled by complex gene networks of signaling pathways. This may explain why the tremendous advances in rice functional genomics research have very limited applications to rice improvement, because phenotypes of complex traits of breeding populations remain largely unpredictable based on information on 'causative' genetic variants at single loci of experimental populations. In this study, we investigated the underlying causes by integrated analyses of the functional relationships and population genomic diversity of a key set of regulatory genes involved in the OsSK41-OsIAA10-OsARF module of rice. We started with the QTL gene *OsSK41* that we cloned previously. *OsSK41* encodes a glycogen synthase kinase GSK3/SHAGGY-like kinase and affects rice grain traits (Hu et al., 2018). We then demonstrated that *OsSK41* negatively regulated the expression of the auxin-responsive gene *OsIAA10* by directly binding to domain II of the OsIAA10 protein and slowing its degradation (Figures 1, 3). We also validated the interactions between the auxin co-receptor complex OsTIR1/OsAFB2 and OsIAA10. Moreover, we successfully determined the relationship between OsSK41 and OsTIR1/OsAFB2 by considering their competitive binding to domain II of OsIAA10 (Figure 4H), which affected the ability of OsSK41 to phosphorylate OsIAA10 and stabilize its expression, and thus indirectly inhibit the activity of its downstream transcriptional activator OsARFs and their regulated downstream response genes. We confirmed experimentally that these OsARFs (OsARF6, OsARF11, OsARF12, OsARF17, OsARF21, OsARF25) interacted directly with OsIAA10; each of the OsARFs can activate many downstream genes responsive to OsIAA10 signaling. The phenotypic evaluation results of the knockout transgenic lines and/or overexpressing lines indicated that the observed phenotypic effects of these genes in the OsSK41-OsIAA10-OsARF module partially overlapped, although both the traits affected and the magnitude of effects on the same grain/yield traits varied (Figure 5). This is not surprising because all their effects on the rice grain and yield traits were achieved indirectly through two subsets of downstream genes/pathways activated by OsARF21 and possibly additional OsARFs such as OsARF6 (Zhang et al., 2018). Moreover, we found that major natural alleles (haplotype combinations) were present at all these regulatory genes, except *OsARF11*, in major rice populations, most of which were differentiated strongly between subspecies *Xian/indica* and *Geng/japonica* and/or between the modern varieties and landraces, indicating they had gone through very different selection pressures during evolution and breeding. Together, our results detected several important aspects about the genetic and molecular bases of rice grain and yield traits regulated by auxin signaling pathways that provide insights into the genetic and molecular bases of complex traits. Important areas were identified for future rice functional genomics research and for developing efficient strategies to improve rice yield traits through various molecular breeding approaches.

Regulation of rice yield traits by the auxin signaling pathways

Auxin is the most important phytohormone that regulates plant growth and development, and almost all the regulatory genes involved in its signaling are expected to influence traits

related to rice productivity and the plant's adaptation to environments. Two large gene families, the *OsIAAs* and *OsARFs*, are key regulatory genes in rice auxin signaling pathways that are known to show tissue/organ- and developmental-specific expression patterns (Song et al., 2009; Wang et al., 2018c). Each of the OsIAAs and one or more of the regulated OsARFs together with specific sets of downstream genes/pathways regulated by the OsARFs form a single and largely independent signaling pathway that regulates a specific set of phenotypes. For example (Figure 5), genes involved in the rice OsSK41-OsIAA10-OsARF module can be conceptually divided into three large functional groups: (I) OsIAA10 and regulators such as OsSK41 and *OsmiR393*, OsTIR1/OsAFB2, and possible transporters of OsIAA10 that function at the level of OsIAA10 signaling; (II) nine OsARFs (OsARF5, OsARF6, OsARF11, OsARF12, OsARF16, OsARF17, OsARF19, OsARF21, OsARF25) that interact directly with OsIAA10 and function as activators plus possible OsARF repressors at the level of transcriptional regulation (Qin et al., 2020); and (III) multiple sets of downstream auxin responsive genes activated or repressed by each of the OsARF activators or repressors that directly control specific biosynthesis/metabolomics pathways and cellular processes and affect a specific suit of phenotypes. Then, several properties of the three groups of genes can be perceived for the phenotypic effects on specific complex traits based on the functional relationships of these genes.

First, *OsARFs* are the key determinants of traits or phenotypes that can be positively regulated in each of the auxin signaling pathways. For example, *OsARF21* positively regulated GL, GW, TGW, and PH, and negatively regulated PN and SNP (Figure 5). Of the nine OsARF activators that interacted directly with OsIAA10. OsARF6 regulated GL and TGW (Qiao et al., 2021); OsARF17 positively regulated rice resistance to virus diseases (Zhang et al., 2020); OsARF12 positively regulated rice root elongation, iron accumulation (Qi et al., 2012), and phosphate homeostasis (Wang et al., 2014); OsARF25 regulated GL (Zhang et al., 2018); and OsARF19 regulated rice floral organ development and plant architecture (Zhang et al., 2015; Zhang et al., 2016). Moreover, OsARF12, OsARF17, and OsARF25 function redundantly to modulate tiller angle (Li et al., 2020). Thus, each OsARF in the OsSK41-OsIAA10-OsARF module regulates a specific suit of phenotypes by activating a specific set of downstream genes that function in specific metabolomic/cellular pathways. However, the current information on what and how many traits are regulated by each of the nine OsARFs remains incomplete. Thus, identifying downstream genes regulated by each of the OsARFs and determining how they are involved in specific metabolomic/cellular pathways leading to specific phenotypes should be an important focus of future rice functional genomics research.

Second, the phenotypic effects of the upstream group I genes involved in auxin signal transduction, such as *OsSK41*, *OsmiR393*, *OsTIR1/OsAFB2*, and *OsIAA10* in the OsSK41-OsIAA10-OsARF module on rice grain and yield traits were the average effects of all the downstream *OsARFs*, including *OsARF21*, *OsARF6*, and other *OsARFs* that affect the same yield traits. This scenario can be extended to include multiple OsIAA signaling pathways, or more broadly multiple OsIAA–OsARF combinations, because the phenotypic effects of different OsIAA signaling pathways on rice grain and yield traits should largely be independent of one another. For example, the OsIAA3–ARF25 combination was reported to positively regulate GL and TGW, and negatively regulate SMP, spikelet fertility, and GYP (Zhang et al., 2018). Specific functional OsIAA–OsARF combinations can be predicted from the tissue/organ- and developmental-specific expression patterns of their commonly regulated downstream genes. Thus, the overall phenotypic effects of auxin signaling pathways on rice grain and yield traits will be the sum of all largely independent OsIAA signaling pathways. An additional layer in the regulation of rice grain and yield traits by group I genes may result from the presence of multiple OsAFBs because different OsAFBs can form different OsTIR1/OsAFBs complexes that regulate IAA signaling. This situation was suggested by our observation that *OsTIR1* and *OsAFB2* affected different sets of grain and yield traits, and *OsTIR1* had much stronger phenotypic effects than *OsAFB2* on the same grain and yield traits (Figure 4).

Third, the regulation of grain/yield traits and differentiated adaptations of subspecies *Xian/indica* and *Geng/japonica* to their respective environments by rice OsIAAs signaling pathways were achieved largely by the rich natural allelic diversity at most regulatory loci of groups I and II in rice populations. The rich natural allelic diversity was evidenced by the presence and strong differentiation of major promoter–CDS haplotype combinations of the *ARFs* in major rice populations, by the strong associations of these combinations with rice grain and yield traits, and by the strong responses of the combinations to artificial selection during breeding (Figures S14–S18). If these major promoter–CDS haplotype combinations indeed have large allelic effects on yield traits, they should be detected as QTLs associated with rice grain yield traits in experimental populations; this remains to be tested. Meanwhile, the functional relationships between or among group I and II loci will be reflected by complex epistatic relationships, and their effects on specific yield traits can be quantified by the theoretical framework in the molecular quantitative genetics theory (Zhang et al., 2011). The properties related to the regulation of rice grain and yield traits by the OsSK41-OsIAA10-OsARF module should largely hold true for complex traits regulated by all OsIAA signaling pathways as well as other phytohormone signaling pathways.

Implications in applying rice functional and population genomics research results to rice improvement

Complex traits, particularly yield traits of rice, are primarily controlled by complex gene networks is auxin signaling pathways, and therefore the phenotypic effects of most, if not all, genes on complex traits are indirect and largely

unpredictable in progenies of breeding populations. Nevertheless, four important observations were noted about the functionality and genetic diversity at the regulatory loci involved in the OsSK41-OsIAA10-OsARF module that have implications in identifying target genes and determining breeding strategies for improving specific target grain yield traits. The first observation was that OsARF activators are key in determining specific phenotypes regulated by each of the auxin signaling pathways; thus, OsARF activators should be target genes for improving specific target traits by appropriate molecular breeding strategies. For example, our functional model (Figure 5) indicates that improved grain yield traits can be more accurately achieved by overexpression of *OsARF21*, and improved resistance to rice viruses can be more accurately achieved by overexpression of *OsARF17*. More dramatic effects on improved yield traits may be achieved by overexpressing/manipulating two or more *OsARFs* simultaneously because their effects on grain yield are expected to be additive. Clearly, it would be ideal if information on the downstream genes/pathways activated by all target *OsARFs* was available. The second observation was that special attention should be paid in selecting 'correct' alleles (gcHaps) of *OsARFs* as target genes in *Xian/indica* and *Geng/japonica* breeding programs because of the presence of subspecific gcHaps at most *OsARFs*. The third observation was that regulatory genes involved in signal transduction of auxin signaling pathways may not be good targets for improving grain yield traits because of their possible pleiotropic effects on many non-target traits. The fourth observation was the rich gene haplotype diversity and the presence of several major gene haplotypes at almost all the regulatory genes, and strong associations of the major gene haplotypes with grain yield traits in the rice populations. This suggests that improvement of single yield traits may be better achieved by searching and pyramiding the 'best' gene haplotype combinations at multiple regulatory genes, particularly the transcription activators. The 'best' allelic combinations for improved grain yield traits may be different in populations *Xian/indica* and *Geng/japonica*, and searching and validation of the "favorable" haplotypes or haplotype combinations that had the "best" yield performances in major rice ecotypes and across major target environments should be an important area to apply results from rice functional genomics research to achieve accelerated genetic gains in future rice improvement programs. Clearly, more accurate manipulation of complex yield traits requires a full understanding of the downstream genes that are positively regulated by OsARF activators as well as the related metabolomics/biosynthetic pathways and affected cellular processes they are associated with. Such information is likely to be obtained experimentally and/or from various omics databases in the public domain because of continuous global efforts in functional genomics research.

MATERIALS AND METHODS

Plant materials and phenotypic assays of transgenic plants

Most of the transgenic plants used in this study were generated from the *Oryza sativa* subsp. *Geng/japonica* cvs. Nipponbare and Zhong Hua 11 (ZH11) as the wild-type backgrounds. All rice materials were evaluated for the following grain yield traits: GL, GW, thousand-grain-weight (TGW), PH, main PL, panicle number per plant (PN), spikelets of main panicle (SMP), spikelets per plant (SNP), and GYP under a long-day environment (May–October) in the experimental fields of Fudan University in Shanghai (31° 11′ N, 121° 29′ E) and under a short-day environment in Hainan (18° 14′ N, 109° 31′ E). Tobacco plants (*Nicotiana benthamiana*) were used for the bimolecular fluorescence complementation and for split-luciferase assays. The tobacco plants were grown in a greenhouse at 26°C under long-day conditions (16-h light/8-h dark) at Fudan University.

Generation of transgenic plants

Generation of CRISPR/Cas9 knockout lines and transformation of overexpression vectors were performed at BioRun Co., Ltd. (Wuhan, China) and Biogle Co., Ltd. (Changzhou, China). Positive transgenic individuals were confirmed by PCR amplification and DNA-sequencing analyses using the primers listed in Table S1.

RNA isolation and qPCR

Total RNA was extracted from leaf samples or young panicles of rice using a FastPure Plant Total RNA Isolation Kit (Vazyme). The qPCR analysis was performed using a Bio-Rad CFX96 real-time PCR system with TB Green Premix Ex Taq II (Takara). *OsUBQ5* or *OsActin1* was used as an internal control for normalization of transcript levels. The relative quantification method ($\Delta\Delta C_t$) was used to evaluate quantitative variation of replicates. All assays were performed with three biological replicates. The PCR primers are listed in Table S2.

Subcellular localization of target genes

To investigate the subcellular localization of the target genes, the fusion construct (*35S*::OsIAA10/OsTIR1-GFP) and control construct (*35S*::GFP) were transformed separately into rice protoplasts. Nucleus marker *35S*::OsPAY1-mCherry was used for the co-localization analysis. The transformed cells were cultured for 14 h then examined using a confocal fluorescence microscope (Leica Microsystems, Mannheim, Germany).

Yeast two-hybrid (Y2H) assays to detect protein–protein interactions of target genes

The full-length CDSs and truncated fragment series of *OsIAA10* and *OsTIR1* were amplified and recombined into the 'prey' pGADT7 vector. Full-length CDSs of *OsSK41* and *OsARFs* were cloned into the 'bait' pGBKT7 vector. All clones

were validated by sequencing and cultured at 30°C for 3–4 days.

BiFC assays

We used the pXY106 vector and pXY104 to construct nYFP-OsIAA10, OsSK41-cYFP, and OsTIR1-cYFP fusion proteins. These combinations of plasmids were transformed into *Agrobacterium tumefaciens* GV3101, and then co-infiltrated into 4–5-week-old tobacco leaves for transient expression. The 35S::PAY1-mCherry nuclear marker was used for the co-localization analysis. Three days after the infiltration, tobacco epidermal leaf cells were observed using a confocal fluorescence microscope. Similarly, the full-length CDS of *OsARF21* was cloned into pXY104 to construct the OsARF21-cYFP fusion protein. Different plasmid combinations were co-transformed into rice protoplasts by polyethylene glycol-mediated transformation. The transformed cells were cultured for 14 h in darkness then examined using a confocal fluorescence microscope.

Glutathione S-transferase (GST) pull-down assays

The full-length CDSs of *OsSK41* and *OsIAA10* were cloned into vectors pGEX4T-1 and vector pCold-transcription factor to construct corresponding fusion proteins with a GST-tag and a His-tag, respectively. In addition, *OsIAA10*-M (mutated) and *OsTIR1* were cloned into vector pGEX4T-1 to construct a fusion protein with a GST-tag. Expression of GST-OsSK41, GST-OsIAA10, GST-OsIAA10-M, GST-OsTIR1, His-OsSK41, in His-OsIAA10 in *E. coli* BL21 (DE3) cells was induced with 0.5 mM isopropyl-β-d-thiogalactoside (IPTG) at 15°C for 16 h. The recombinant proteins were extracted with extraction buffer (50 mM Tris–HCl, 150 mM NaCl, 1 mM EDTA, 10% glycerol, 0.5% Triton X-100, 1 mM PMSF, 1/100 protease inhibitor) after ultrasonic decomposition. The GST-tagged and His-tagged proteins were purified using glutathione sefinose resin and Ni-NTA agarose beads, respectively.

Split-luciferase assays

We used pCAMBIA2300-cLUC and pCAMBIA2300-nLUC to construct cLUC-OsSK41, OsIAA10-nLUC, and cLUC-OsARF21 recombinant plasmids and empty vector controls, which were transformed into *Agrobacterium* strain GV3101. Different combinations of *A. tumefaciens* harboring the nLUC or cLUC fusion plasmid were infiltrated into tobacco leaves. Three days after infiltration, luciferin solution (2.5 mM, 0.1% Triton X-100) was sprayed onto the leaves. After approximately 5 min of dark treatment, the luciferase luminescence signals were imaged using an *in vivo* plant imaging system (NIGHTSHADE LB 985).

Yeast three-hybrid assays and determination of β-galactosidase activity

We used the previously constructed AD-OsARF21 as Prey. The full-length CDS of *OsIAA10* was amplified and recombined into the MCS I location of a pBridge vector to construct Bait I. To construct Bait II, the CDS of *OsSK41* was cloned into the MCS II location of Bait I. Each bait and prey pair was co-introduced into yeast strain AH109, then the monoclones were selected and incubated at 29°C for 3 days. Yeast cells were collected and re-suspended in 600 µl Z-buffer (60 mM Na_2HPO_4, 40 mM NaH_2PO_4, 10 mM KCl, 1 mM $MgSO_4$, 50 mM β-mercaptoethanol, pH 7.0), then placed in liquid nitrogen for 1 min, followed by 37°C for 3 min (repeated four times). After equilibration at 30°C for 5 min, 120 µl of 4 mg/ml o-nitrophenyl-β-d-galactoside was added to the mixture and thoroughly vortexed before incubation at 30°C. The reaction was stopped by adding 400 µl 1 M Na_2CO_3. The relative β-galactosidase activity unit was calculated as follows: 1,000 × D420 nm/D600 nm × reaction time (min) × 0.1 × dilution factor.

Phosphorylation assays

We incubated 2 mg of GST-OsSK41 and 2 mg of His-OsIAA10 in a kinase reaction buffer (20 mM Tris-HCl [pH 7.5], 12 mM $MgCl_2$, 2 mM ATP) at 30°C for 30 min. The reaction was stopped by adding 2× SDS loading buffer and boiling for 10 min at 95°C. The phosphorylated samples were further separated by 8% SDS-PAGE (sodium dodecyl sulfate-polyacrylamide gel electrophoresis) containing 20 µM Phos-tag and 40 µM $MnCl_2$. For phosphopeptide identification, the separated phosphorylated proteins in the gel were collected and used for an LC-MS/MS analysis.

Determining *OsIAA10* protein stability

To determine *in vitro* protein stability, fresh total protein extracts were prepared from rice leaves using a Plant Active Protein Extraction Kit (Sangon Biotech) to establish the cell-free degradation mixture. Then, mixing unmutated His-OsIAA10 with GST-OsSK41 or mutated GST-OsIAA10-M with His-OsSK41, which was then incubated at 30°C for 80 min. Samples were collected at 0, 20, 40, 60, and 80 min for the standard immunoblot assays.

Scanning electron microscopy

The epidermal cells were examined with a scanning electron microscope.

Population genetic analysis

The gene CDS haplotypes (gcHaps) and gene promoter haplotypes (gpHaps) of *OsIAA10*, *OsSK41*, *OsTIR1*, *OsAFB2*, and *OsARF21* in the 3,000 rice genomes (3KRG) dataset were detected using all the single-nucleotide polymorphisms within their CDS regions and 1-kb regions upstream of the start codon (Wang et al., 2020; Zhang et al., 2021), respectively. To determine the phenotypic differences among the major haplotypes (present in ≥30 rice accessions) of the six target genes associated with grain yield traits including TGW, GL, GW, and the GL/GW ratio previously reported by Niu et al. (2021), we performed one-way analysis of variance followed by multiple comparisons among the major haplotypes by least significant difference tests using the agricolae package in R. Then, Shannon's equitability (E_H) (Sheldon, 1969) was estimated using the haplotype data to compare the gene diversity among different rice populations.

The frequencies of the favorable haplotypes (defined as those associated with the highest trait values) at the target genes in the modern varieties and landraces in populations *Xian/indica* and *Geng/japonica* were compared using chi-square tests in R, to determine if specific haplotypes at any of the six target genes had undergone strong artificial selection during modern breeding programs.

ACKNOWLEDGEMENTS

This work was supported by the Innovation Program of Shanghai Municipal Education Commission (2023ZKZD05), the National Natural Science Foundation of China (31971918, U21A20214), and the Shanghai Science and Technology Innovation Action Plan Project (22N11900200).

CONFLICTS OF INTEREST

The authors have no conflict of interest to declare.

AUTHOR CONTRIBUTIONS

X.L., Z.L., and F.Z. planned the research and revised the manuscript; J.Y. and L.C. directed the research; F.M., F.Z., and Y.Z. performed the research and wrote the manuscript; D.L., P.Y., Y.W., Z.H., X.Z., J.H., F.N., M.L., S.H., J.C., X.Y., Y.Y., and S.W. analyzed parts of the data; H.B. provided some of the seeds. All authors read and approve of the manuscript.

Edited by: Letian Chen, South China Agricultural University, China

Received Jan. 30, 2023; **Accepted** Mar. 20, 2023; **Published** Mar. 20, 2023

OO: OnlineOpen

REFERENCES

Basunia, M.A., Nonhebel, H.M., Backhouse, D. and McMillan, M. (2021). Localised expression of OsIAA29 suggests a key role for auxin in regulating development of the dorsal aleurone of early rice grains. Planta **254:** 40.

Bian, H., Xie, Y., Guo, F., Han, N., Ma, S., Zeng, Z., Wang, J., Yang, Y. and Zhu, M. (2012). Distinctive expression patterns and roles of the miRNA393/TIR1 homolog module in regulating flag leaf inclination and primary and crown root growth in rice (*Oryza sativa*). New Phytol. **196:** 149–161.

Gao, X., Zhang, J.Q., Zhang, X., Zhou, J., Jiang, Z., Huang, P., Tang, Z., Bao, Y., Cheng, J., Tang, H., et al. (2019). Rice qGL3/OsPPKL1 functions with the GSK3/SHAGGY-like kinase OsGSK3 to modulate brassinosteroid signaling. Plant Cell **31:** 1077–1093.

Gray, W.M., Kepinski, S., Rouse, D., Leyser, O. and Estelle, M. (2001). Auxin regulates SCFTIR1-dependent degradation of AUX/IAA proteins. Nature **414:** 271–276.

Guo, F., Huang, Y., Qi, P., Lian, G., Hu, X., Han, N., Wang, J., Zhu, M., Qian, Q. and Bian, H. (2021). Functional analysis of auxin receptor OsTIR1/OsAFB family members in rice grain yield, tillering, plant height, root system, germination, and auxinic herbicide resistance. New Phytol. **229:** 2676–2692.

Hu, Z., Lu, S.J., Wang, M.J., He, H., Sun, L., Wang, H., Liu, X.H., Jiang, L., Sun, J.L., Xin, X., et al. (2018). A novel QTL qTGW3 encodes the GSK3/SHAGGY-like kinase OsGSK5/OsSK41 that interacts with OsARF4 to negatively regulate grain size and weight in rice. Mol. Plant **11:** 736–749.

Ishimaru, K., Hirotsu, N., Madoka, Y., Murakami, N., Hara, N., Onodera, H., Kashiwagi, T., Ujiie, K., Shimizu, B.i, Onishi, A., et al. (2013). Loss of function of the IAA-glucose hydrolase gene TGW6 enhances rice grain weight and increases yield. Nat. Genet. **45:** 707–711.

Jiang, H., Zhang, A., Liu, X. and Chen, J. (2022). Grain size associated genes and the molecular regulatory mechanism in rice. Int. J. Mol. Sci. **23:** 3169–3179.

Jin, L., Qin, Q., Wang, Y., Pu, Y., Liu, L., Wen, X., Ji, S., Wu, J., Wei, C., Ding, B., et al. (2016). Rice dwarf virus P2 protein hijacks auxin signaling by directly targeting the rice OsIAA10 protein, enhancing viral infection and disease development. PLoS Pathog. **12:** e1005847.

Li, Y., Li, J.L., Chen, Z.H., Wei, Y., Qi, Y.H., and Wu, C.Y. (2020). OsmiR167a-targeted auxin response factors modulate tiller angle via fine-tuning auxin distribution in rice. Plant Biotechnol. J. **18:** 2015–2026.

Li, Z.K. and Zhang, F. (2013). Rice breeding in the post-genomics era: From concept to practice. Curr. Opin. Plant Biol. **16:** 261–269.

Lyu, J., Wang, D., Duan, P., Liu, Y., Huang, K., Zeng, D., Zhang, L., Dong, G., Li, Y., Xu, R., et al. (2020). Control of grain size and weight by the GSK2-LARGE1/OML4 pathway in rice. Plant Cell **32:** 1905–1918.

Müllender, M., Varrelmann, M., Savenkov, E.I. and Liebe, S. (2021). Manipulation of auxin signalling by plant viruses. Mol. Plant Pathol. **22:** 1449–1458.

Nakamura, A., Umemura, I., Gomi, K., Hasegawa, Y., Kitano, H., Sazuka, T., and Matsuoka, M. (2006). Production and characterization of auxin-insensitive rice by overexpression of a mutagenized rice IAA protein. Plant J. **46:** 297–306.

Niu, Y., Chen, T., Wang, C., Chen, K., Shen, C., Chen, H., Zhu, S., Wu, Z., Zheng, T., Zhang, F., et al. (2021). Identification and allele mining of new candidate genes underlying rice grain weight and grain shape by genome-wide association study. BMC Genomics **22:** 602.

Qi, Y., Wang, S., Shen, C., Zhang, S., Chen, Y., Xu, Y., Liu, Y., Wu, Y. and Jiang, D. (2012). OsARF12, a transcription activator on auxin response gene, regulates root elongation and affects iron accumulation in rice (*Oryza sativa*). New Phytol. **193:** 109–120.

Qiao, J., Jiang, H., Lin, Y., Shang, L., Wang, M., Li, D., Fu, X., Geisler, M., Qi, Y., Gao, Z., et al. (2021). A novel miR167a-OsARF6-OsAUX3 module regulates grain length and weight in rice. Mol. Plant **14:** 1683–1698.

Qin, Q., Li, G., Jin, L., Huang, Y., Wang, Y., Wei, C., Xu, Z., Yang, Z., Wang, H. and Li, Y. (2020). Auxin response factors (ARFs) differentially regulate rice antiviral immune response against rice dwarf virus. PLoS Path. **16:** e1009118.

Sheldon, A.L. (1969). Equitability indices: Dependence on the species count. Ecology **50:** 466–467.

Shen, C., Wang, S., Bai, Y., Wu, Y., Zhang, S., Chen, M., Guilfoyle, T.J., Wu, P. and Qi, Y. (2010). Functional analysis of the structural domain of ARF proteins in rice (*Oryza sativa* L.). J. Exp. Bot. **61:** 3971–3981.

Song, Y., Wang, L. and Xiong, L. (2009). Comprehensive expression profiling analysis of OsIAA gene family in developmental processes and in response to phytohormone and stress treatments. Planta **229:** 577–591.

Tong, H., Liu, L., Jin, Y., Du, L., Yin, Y., Qian, Q., Zhu, L. and Chu, C. (2012). DWARF AND LOW-TILLERING acts as a direct downstream target of a GSK3/SHAGGY-like kinase to mediate brassinosteroid responses in rice. Plant Cell **24:** 2562–2577.

Wang, C.C., Yu, H., Huang, J., Wang, W.S., Faruquee, M., Zhang, F., Zhao, X.Q., Fu, B.Y., Chen, K., Zhang, H.L., et al. (2020). Towards a deeper haplotype mining of complex traits in rice with RFGB v2.0. Plant Biotechnol. J. **18:** 14–16.

Wang, L., Yang, Z., Zhang, B., Yu, D., Liu, J., Gong, Q., Qanmber, G., Li, Y., Lu, L., Lin, Y., et al. (2018a). Genome-wide characterization and phylogenetic analysis of GSK gene family in three species of cotton: Evidence for a role of some GSKs in fiber development and responses to stress. BMC Plant Biol. **18:** 330.

Wang, S., Zhang, S., Sun, C., Xu, Y., Chen, Y., Yu, C., Qian, Q., Jiang, D.-A. and Qi, Y. (2014). Auxin response factor (OsARF12), a novel regulator for phosphate homeostasis in rice (Oryza sativa). New Phytol. **201:** 91–103.

Wang, W., Mauleon, R., Hu, Z., Chebotarov, D., Tai, S., Wu, Z., Li, M., Zheng, T., Fuentes, R.R., Zhang, F., et al. (2018b). Genomic variation in 3,010 diverse accessions of Asian cultivated rice. Nature **557:** 43–49.

Wang, Y., Zhang, T., Wang, R. and Zhao, Y. (2018c). Recent advances in auxin research in rice and their implications for crop improvement. J. Exp. Bot. **69:** 255–263.

Wing, R.A., Purugganan, M.D. and Zhang, Q. (2018). The rice genome revolution: From an ancient grain to Green Super Rice. Nat. Rev. Genet. **19:** 505–517.

Worley, C.K., Zenser, N., Ramos, J., Rouse, D., Leyser, O., Theologis, A., and Callis, J. (2000). Degradation of Aux/IAA proteins is essential for normal auxin signalling. Plant J. **21:** 553–562.

Xia, K., Wang, R., Ou, X., Fang, Z., Tian, C., Duan, J., Wang, Y. and Zhang, M. (2012). OsTIR1 and OsAFB2 downregulation via OsmiR393 overexpression leads to more tillers, early flowering and less tolerance to salt and drought in rice. PLoS ONE **7:** e30039.

Youn, J.H. and Kim, T.W. (2015). Functional insights of plant GSK3-like kinases: Multi-taskers in diverse cellular signal transduction pathways. Mol. Plant **8:** 552–565.

Zhang, F., Wang, C., Li, M., Cui, Y., Shi, Y., Wu, Z., Hu, Z., Wang, W., Xu, J. and Li, Z. (2021). The landscape of gene-CDS-haplotype diversity in rice (*Oryza sativa* L.): Properties, population organization, footprints of domestication and breeding, and implications in genetic improvement. Mol. Plant **14:** 787–804.

Zhang, F., Zhai, H., Paterson, A.H., Xu, J., Gao, Y., Zheng, T., Wu, R., Fu, B., Ali, J. and Li, Z. (2011). Dissecting genetic networks underlying complex phenotypes: The theoretical framework. PLoS One **6:** e14541.

Zhang, H., Li, L., He, Y., Qin, Q., Chen, C., Wei, Z., Tan, X., Xie, K., Zhang, R., Hong, G., et al. (2020). Distinct modes of manipulation of rice auxin response factor OsARF17 by different plant RNA viruses for infection. P. Natl. Acad. Sci. U.S.A. **117:** 9112–9121.

Zhang, S., Wang, S., Xu, Y., Yu, C., Shen, C., Qian, Q., Geisler, M., Jiang, D.A. and Qi, Y. (2015). The auxin response factor, OsARF19, controls rice leaf angles through positively regulating OsGH3-5 and OsBRI1. Plant Cell Environ. **38:** 638–654.

Zhang, S., Wu, T., Liu, S., Liu, X., Jiang, L. and Wan, J. (2016). Disruption of OsARF19 is critical for floral organ development and plant architecture in rice (*Oryza sativa* L.). Plant Mol. Biol. Rep. **34:** 748–760.

Zhang, Z., Li, J., Tang, Z., Sun, X., Zhang, H., Yu, J., Yao, G., Li, G., Guo, H., Li, J., et al. (2018). Gnp4/LAX2, a RAWUL protein, interferes with the OsIAA3–OsARF25 interaction to regulate grain length via the auxin signaling pathway in rice. J. Exp. Bot. **69:** 4723–4737.

SUPPORTING INFORMATION

Additional Supporting Information may be found online in the supporting information tab for this article: http://onlinelibrary.wiley.com/doi/10.1111/jipb.13484/suppinfo

Figure S1. The yeast-two-hybrid assay showing OsSK41 interacts with OsIAA10 in yeast

Figure S2. RNA-seq analysis in wild-type Nipponbare and *OsSK41* knockout lines

Figure S3. The expression patterns of *OsIAA10* and *OsSK41* in different tissues of wild-type Nipponbare

Figure S4. Phenotypes of the T_0 generation of *OsIAA10* knockout lines in Hainan

Figure S5. Phenotypic comparison for grain and yield traits between the *OsIAA10* knockout lines and wild type in the ZH11 and Nipponbare genetic background assessed in Hainan (short-day environment)

Figure S6. Phenotypic comparison for grain and yield traits between the *OsTIR1* knockout lines, *OsAFB2* knockout lines, *OsmiR393* overexpression lines and wild-type in the Nipponbare genetic background assessed in Hainan (short-day environment)

Figure S7. Yeast two-hybrid verification for the absence of interaction between OsSK41 and OsTIR1

Figure S8. Yeast two-hybrid verification of the interactions between OsIAA10 and OsARF activators

Figure S9. Determination of the functional relationships between *OsIAA10*, *OsSK41* and *OsARF21*

Figure S10. Phenotypic comparison of *OsARF21* knockout lines and overexpression lines with wild type in Shanghai

Figure S11. Phenotypic comparison of other *OsARF21* knockout lines and wild type in Shanghai

Figure S12. Phenotypic comparison for grain and yield traits between the *OsARF21* knockout lines and wild-type in the Nipponbare genetic background assessed in Hainan (short-day environment)

Figure S13. The role of OsSK41 in the interaction of OsIAA10 with OsARF21 verified by yeast three-hybrid

Figure S14. Genetic diversity of *OsSK41*/*OsGSK5* in rice

Figure S15. Genetic diversity of *OsIAA10* in rice

Figure S16. Genetic diversity of *OsTIR1* in rice

Figure S17. Genetic diversity of *OsAFB2* in rice

Figure S18. Genetic diversity of *OsARF21* in rice

Figure S19. Graphical haplotypes of *OsSK41*/*OsGSK5*, *OsIAA10*, *OsTIR1*, *OsAFB2*, *OsAFB4* and *OsARF21* for 1,483 rice accessions with phenotype of seven traits

Table S1. Primers used to confirm knockout lines

Table S2. Primers used for the qPCRs

Table S3. Gene CDS haplotype diversity (Shannon's equitability E_H) at seven genes involved in the auxin signaling pathways in major rice populations

Table S4. Gene promoter (upstream 1 kb) haplotype diversity (Shannon's equitability E_H) at seven genes involved in the auxin signaling pathways in major rice populations

Scan using WeChat with your smartphone to view JIPB online

Scan with iPhone or iPad to view JIPB online